I. KUKUŁA*, H. BALA*

EFFECT OF POWDER GRANULATION ON HYDROGEN TRANSPORT RATE AND HYDROGEN SOLUBILITY IN LaNi$_5$-PARAFFIN COMPOSITE MATERIAL

WPŁYW GRANULACJI PROSZKU NA SZYBKOŚĆ TRANSPORTU I ROZPUSZCZALNOŚĆ WODORU W MATERIALE KOMPOZYTOWYM: PROSZEK LaNi$_5$-PARAFINA

On the basis of potentiostatic discharge method, the diffusion rate of atomic hydrogen as well as its solubility in LaNi$_5$ crystal lattice have been evaluated for three LaNi$_5$ powder – paraffin composite electrodes, with different LaNi$_5$ powder particle diameters: $0 - 20$ μm, $20 - 50$ μm and $50 - 100$ μm. The chronoamperommetric tests have been carried out in strong alkaline (6 M KOH), deaerated solution, at 25°C. Apparent hydrogen diffusion coefficients have been determined using Crank's spherical diffusion model. It has been shown, that increase of particle size is prone to increase of hydrogen apparent diffusion coefficient and to decrease of hydrogen concentration in the solid phase. To explain the granulation effect on hydrogenation ability parameters, the inhibition of hydrogen transport by surfacial corrosion products present on powder particles has been assumed.

Keywords: NiMH, LaNi$_5$ powder, hydrogenation, hydrogen diffusion

Za pomocą potencjostatycznej metody rozładowania oceniono szybkość dyfuzji atomowego wodoru i jego rozpuszczalność w sieci krystalicznej LaNi$_5$ dla trzech elektrod kompozytowych: proszek LaNi$_5$ – parafina przy różnych średnich rozmiarach cząstek LaNi$_5$: $0 - 20$ μm, $20 - 50$ μm i $50 - 100$ μm. Badania chronoamperometryczne przeprowadzono w silnie zasadowym (6 M KOH), odpowietrzonym roztworze, przy 25°C. Pozorne współczynniki dyfuzji wodoru wyznaczono wykorzystując model sferycznej dyfuzji Crank'a. Pokazano, że wzrost rozmiarów cząstek proszku prowadzi do wzrostu wartości pozornego współczynnika dyfuzji w fazie stałej. Dla wytłumaczenia wpływu granulacji na parametry opisujące zdolność wodorowania założono, że transport atomowego wodoru ulega spowolnieniu wskutek obecności powierzchniowych produktów korozji na cząstkach proszku.

1. Introduction

Rare earth element (R) – transition metal (T) intermetallic compounds of general formulae RT$_5$, RT$_3$ and R$_2$T$_7$ are being used as negative electrodes in nickel-metal hydride (NiMH) batteries because of their ability to store large amounts of hydrogen [1-4]. Among these compounds LaNi$_5$ with CaCu$_5$ type structure and alloys on its base attract particularly much attention [4-6]. In order to improve hydrogen capacity, kinetics of charge/discharge processes and corrosion resistance, both La and Ni can be replaced by other elements, e.g. La by Mm (mischmetal), Ce, Pr, Nd, Zr or Hf and Ni by Al, Mn, Si, Zn, Cr, Fe, Cu or Co [4,7-10]. In practical applications LaNi$_5$ type alloys are pulverized with a use of many different methods [4,11]. The powder particles are often microencapsulated by more noble metals which prevents material's corrosion and mechanical degradation [12,13], and usually are mixed with Ni or Cu powder additives to enhance electrical and mechanical properties of the electrode [4,14]. To prepare negative LaNi$_5$-type electrodes with a satisfactory performance, the alloy particles are mixed with 0,1 − 10 wt % of different kind of binders (e.g. polyacrylates, poly(tetrafluoroethylene), poly(vinyl alcohol), carboxymethyl cellulose, epoxy resin etc. [4,15-16]). Authors of the present paper have indicated a number of advantages at using paraffin as a binder for LaNi$_5$ alloy particles consolidation [17]. Such composite electrodes show much better hydrogen absorption/desorption ability as compared with solid alloys [15,16].

The charge-discharge properties of hydrogen storage electrodes are strongly limited by atomic hydrogen transport rate within crystal lattice of metal hy-

* CZESTOCHOWA UNIVERSITY OF TECHNOLOGY, DEPARTMENT OF CHEMISTRY, 42-200 CZĘSTOCHOWA, 19 ARMII KRAJOWEJ AV., POLAND

dride materials. The mechanism of hydrogen transport across the LaNi$_5$-type alloy particles includes both random walk of individual atoms (Einstein diffusion) or as a net flux caused by concentration gradient (Fick's diffusion) [4,18]. The most important factor describing hydrogen diffusion rate within composite LaNi$_5$-type powder electrode is apparent diffusion coefficient ($\overline{D}_H$). There exists many experimental methods to determine $\overline{D}_H$ [19], however, there appear great discrepancies in $\overline{D}_H$ results reported not only by various authors but by the same authors applying different methods as well (e.g. compare, paper of Khaldi et al [20] in which $\overline{D}_H$, depending on experimental method, varies over 3 orders of magnitude for the same material, at room temperature).

For powdered hydrogen storage materials the potentiostatic discharge (chronoamperommetric) method is applied most frequently [18,21,22]. The method is based on Crank's diffusion model [23,24] that considers semi-infinite diffusion of atomic hydrogen leaving spherical LaNi$_5$ particle, initially charged cathodically. Assuming uniform initial hydrogen concentration in the bulk of particle, $C_{H,o}$ and the hydrogen surface concentration, $C_{H,s}$, the anodic current of hydrogen oxidation (I) depends on discharge time (t) in the following way:

$$\log \frac{I}{m_M} = \log \frac{6F\overline{D}_H(C_{H,o} - C_{H,s})}{da^2} - \frac{\pi^2}{2,303}\frac{\overline{D}_H}{a^2}t \quad (1)$$

where m_M is hydrogen storage alloy mass in the electrode [g], d – is the alloy density [g·cm^{-3}], a – the mean radius of alloy particle [cm], F – Faraday constant [96500 A·s·mol^{-1}] and $\overline{D}_H$ – apparent (effective) diffusion coefficient [cm^2·s^{-1}]. In Eq. (1) both hydrogen concentrations are expressed in [mol·cm^{-3}] and I/m_M fraction denotes discharge current density (i), expressed in [A·g^{-1}]. As it results from Eq. (1), at constant anodic potential, usually ~−0.3 V (vs HgO/Hg), and after comparatively long discharge time (after which $C_{H,s} = 0$), the linear relationship between log$i$ and t should exist. The slope of the straight line allows to determine the $\frac{\overline{D}_H}{a^2}$ value and then, hydrogen diffusion coefficient.

The purpose of this paper was to calculate hydrogen diffusion coefficient in LaNi$_5$-paraffin composite electrode on the basis of Crank's model.

At it is known, LaNi$_5$ alloy reacts with oxygen and traces of water steam present in air and its surface covers with a passive layer – the corrosion product consisting mainly of La(OH)$_3$ [25,26]. It may expect that part of corrosion products in the powder alloy increases with the LaNi$_5$ particle decrease and, thus, the passive layer should limit the transport of hydrogen in the powder based composite material. Taking into account passivation of LaNi$_5$ compound particles it is important to check, whether mean particle radius influences the apparent diffusion coefficient $\overline{D}_H$. In present paper the hydrogen diffusion coefficients have been determined using potentiostatic discharge method for three different LaNi$_5$ powder particle sizes.

2. Experimental

Electrochemical (chronoamperommetric) measurements were carried out using CHI 1140A (Austin, Texas, USA) potentiostat in a teflon, 50 cm^3 cell equipped with a working LaNi$_5$-paraffin composite electrode, HgO/Hg reference electrode with Luggin's capillary and Au – counter electrode. The LaNi$_5$ powders were obtained by vibration milling (Yellow Line A 10 mill) of 99.9% LaNi$_5$ alloy (Alfa Aesar) and by powder sieve separation into three fractions: 0 – 20 μm (powder A), 20 – 50 μm (powder B) and 50 – 100 μm (powder C). The working electrode pellets were made by thorough mixing of LaNi$_5$ powder (90% wt), and paraffin (10 % wt). The dense paste was compacted in a temperature of 70 – 80°C under 2 – 3 MPa in a $\emptyset$ = 5 mm and h = 1 mm nette of the working cap. The mass of LaNi$_5$ powder in each pellet was 0,040 g, irrespectively of powder granulation. Fig. 1 presents morphology of the tested composite electrodes.

The electrolyte was deaerated (Ar-saturated) 6 M KOH solution (25°C). The powder composite electrodes (A, B or C) were cathodically charged for 30 mins at 5 mA·g^{-1} and then discharged at a constant potential −0.3 V versus HgO/Hg, with registration of anodic current changes with discharge time.

3. Experimental results and discussion

Figure 2 presents the typical semilogarithmic plots of anodic current-time responses (log$I$ = f(t)) observed at three composite electrodes (made of A, B and C LaNi$_5$ powders) after the potential was stepped from cathodic charging (corresponding to i_c = 5 mA·g^{-1}) to anodic discharging (−0.3 V versus HgO/Hg).
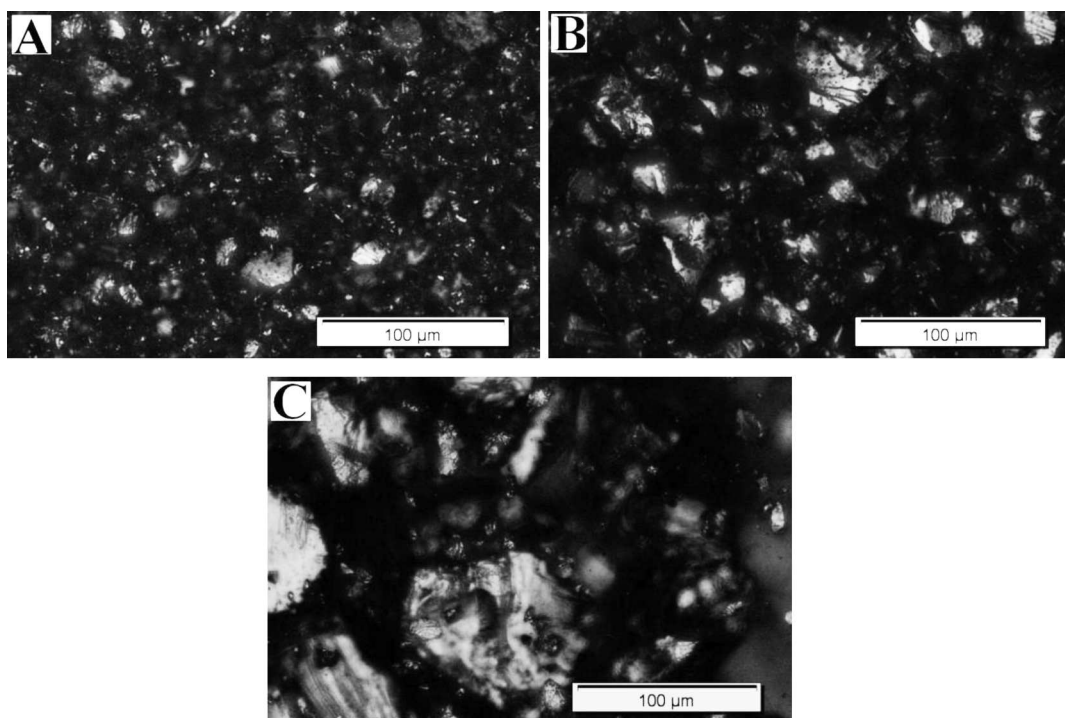
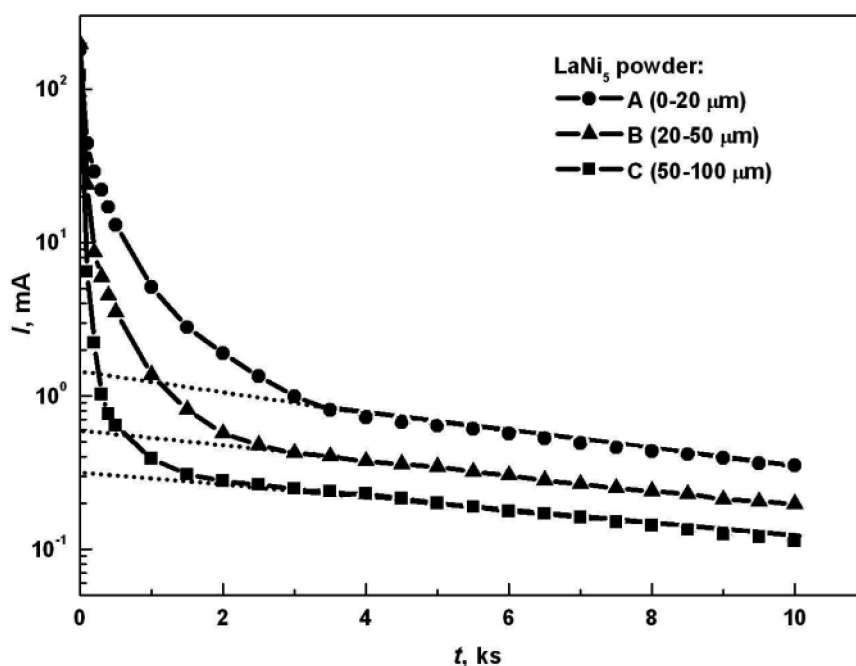Fig. 1. Morphology of three composite electrodes (made of A, B and C LaNi$_5$ powders)

Fig. 2. Chronoamperommetric curves for three composite electrodes (made of A, B and C LaNi$_5$ powders) at constant discharge potential, $E = -0,3$ V (6 M KOH, 25°C, Ar)

Observation of the $\log I = f(t)$ plots allows distinguish the current responses in two time domains. The first one is the time region up to 1.5 – 3 ks in which the current decreases rapidly and the second one is the time >1.5 – 3 ks in which the $\log I$ decreases in a linear fashion. As discussed in papers [21,22], the current responses at the longer times can be treated as the finite diffusion of H-atoms inside the solid particles using a Crank's spherical diffusion model. This way, slopes of linear segments of $\log I = f(t)$ curves are a measure of diffusion coefficients:

$$\left(\frac{\partial \log I}{\partial t}\right)_{E=-0.3V} = -\frac{\pi^2}{2,303} \cdot \frac{\overline{D}_H}{a^2} \qquad (2)$$

The calculated values of $\overline{D}_H$ found on the basis of slopes resulting from Fig. 2 are summarized for the tested powder granulations in Table 1.

TABLE 1

Slopes of rectilinear segments of chronoamperommetric responses and calculated apparent diffusion coefficient for three tested LaNi$_5$-paraffin composite electrodes with different particle size

Powder notation	Powder fraction	Average particle radius a [cm]	$\frac{\pi^2}{2,303} \cdot \frac{\overline{D}_H}{a^2}$ [s^{-1}]	$\overline{D}_H$ [cm^2·s^{-1}]
A	$<20\ \mu m$	$5.0 \cdot 10^{-4}$	$5.6 \cdot 10^{-5}$	$3.2 \cdot 10^{-12}$
B	$20-50\ \mu m$	$1.7 \cdot 10^{-3}$	$4.4 \cdot 10^{-5}$	$2.9 \cdot 10^{-11}$
C	$50-100\ \mu m$	$3.8 \cdot 10^{-3}$	$3.3 \cdot 10^{-5}$	$1.1 \cdot 10^{-10}$

As it results from Table 1, the apparent $\overline{D}_H$ values decrease with particle radius decrease. It should be mentioned that the values on the order of 10^{-10} cm^2·s^{-1} are cited for LaNi$_5$ type alloy $\overline{D}_H$ coefficient most frequently [4, 27].

It is also interesting that for greater LaNi$_5$ type particles (˜200 μm) the $\overline{D}_H$ values were found to be even on the order of $10^{-9}-10^{-8}$ cm^2·s^{-1} [21]. In paper [19] we pointed out on unreliable average radius of powder particles as the main source of experimental errors for determination of hydrogen diffusion coefficient. The actual diffusion coefficient value (D_H) describes the transport rate of H-atoms in LaNi$_5$ crystal lattice, so it should not depend on particle dimensions. However, the apparent coefficient ($\overline{D}_H$) includes also hydrogen transport across particle surfacial layers, among which the natural passive layer formed at the stage of milling as well as the layers produced during alloy contact with KOH solution seem to be obvious obstacles for hydrogen diffusion. The passive layers consist mainly of La(OH)$_3$ [25,26,28,29] and the preferential oxidation of lanthanum is prone to formation of Ni-rich (and La-poor) sublayers, situated directly under passive layers. The tremendous role of surfacial layers in H transport rate is especially distinct for very small LaNi$_5$ particles, since the thickness of passive layers begins to be comparable with average diameter of such particles.

Apart from evaluation of H-atoms diffusion rate within LaNi$_5$ powder particles, the Eq. 1 allows to find the hydrogen concentration in the considered composite material after cathodic charging. As it was discussed in our previous paper [19], extrapolation of rectilinear segment of the chronoamperommetric curve to $t = 0$ corresponds to the pure diffusion control of the hydro-

gen oxidation process, so the $C_{H,s} = 0$, and from Eq. 1 we get after some transformations:

$$C_{H,o} = \frac{da^2 I_{a,0}}{6F\overline{D}_H m_M} \qquad (3)$$

where $I_{a,0}$ is anodic current of hydrogen oxidation found by extrapolation of the rectilinear segment to $t = 0$ (compare Fig. 2). Taking into account that $m_M = 0.040$ g and alloy density is 8.0 g·cm^{-3} [20], one can calculate the initial hydrogen concentration for particular granulations of LaNi$_5$ material. The corresponding results of calculations are presented in Table 2.

TABLE 2

Extrapolated $I_{a,0}$ values and initial hydrogen concentration in cathodically charged ($Q_c = 432$ A·s·g^{-1}) LaNi$_5$ powder-paraffin composite electrodes with different mean particle radii

Powder notation (particle radius, [cm])	$I_{a,0}$ [A]	$\frac{\overline{D}_H}{a^2}$ [s^{-1}]	$C_{H,o}$ [mol·cm^{-3}]
A ($5.0 \cdot 10^{-4}$)	$13 \cdot 10^{-4}$	$1.3 \cdot 10^{-5}$	0.034
B ($1.7 \cdot 10^{-3}$)	$6.0 \cdot 10^{-4}$	$1.0 \cdot 10^{-5}$	0.021
C ($3.8 \cdot 10^{-3}$)	$3.1 \cdot 10^{-4}$	$0.78 \cdot 10^{-5}$	0.014

At it is easy to prove, for saturation of 1 g of LaNi$_5$ with hydrogen to the composition of LaNi$_5$H$_n$, the following charge is necessary:

$$Q_{c,max} = \frac{F \cdot n}{M_{LaNi_5}} \qquad (4)$$

Substituting $F = 96500$ A·s·mol^{-1}, $n = 6$ and $M_{LaNi_5} = 432.4$g · mol^{-1} we get $Q_{c,max} = 1340$ A·s·g^{-1}. Assuming that 100% of reduced hydrogen enters LaNi$_5$ crystal lattice, the maximum hydrogen concentration [mol·cm^{-3}] in hydrogen saturated LaNi$_5$ compound (formula LaNi$_5$H$_6$ [4,30]) is:

$$C_{H,max} = \frac{6 \cdot 8,0g \cdot cm^{-3}}{432.4g \cdot mol^{-1}} = 0.11 mol \cdot cm^{-3} \qquad (5)$$

In experimental conditions assumed in this paper, the cathodic charge applied (432 A·s·g^{-1}) allows to achieve $C_{H,o} = 0.11 \cdot \frac{432}{1340} = 0.035$ mol·cm^{-3}. The value obtained for powder A (0.034 mol·cm^{-3} – compare Table 2) is in good agreement with above predictions. However, for greater particle size (powders B and C), concentration of H atoms directly after charging, is $2-3$ times smaller as compared to $C_{H,o}$ value found for sample A. Apparently, saturation of LaNi$_5$ particles with H-atoms is the easier, the smaller mean particle radius.

4. Conclusions

1. Dimensions of LaNi$_5$ particles in LaNi$_5$–paraffin composite materials strongly influence both hydrogen diffusion rate and hydrogen solubility in the LaNi$_5$-based material; the greater mean particle radius, the greater apparent hydrogen diffusion coefficient, and the smaller hydrogen solubility in LaNi$_5$ crystal lattice.

2. Decrease of hydrogen diffusion coefficients with decrease of mean LaNi$_5$ particle radius can be explained by LaNi$_5$ powder material passivation (particle coverage with La(OH)$_3$-rich corrosion products) and formation of La-poor sublayers directly under passive layers.

REFERENCES

[1] M. Tliha, H. Mathlouthi, J. Lamloumi, A. Percheron-Guegan, J. Alloys Comp. **436**, 221 (2007).

[2] R. Li, J. Wu, H. Su, S. Zhou, J. Alloys Comp. **421**, 258 (2006).

[3] C. Iwakura, M. Matsuoka, Prog. Batteries and Battery Mater. **10**, 81 (1991).

[4] J. Kleperis, G. Wójcik, A. Czerwiński, J. Skowronski, M. Kopczyk, M. Bełtowska-Brzezińska, J.Solid State Electrochem. **5**, 229 (2001).

[5] S. Seta, H. Uchida, J. Alloys Comp. **231**, 448 (1995).

[6] C. Bordeaux, F. Bernard, N. Gérard, Int. J. Hydr. Energy **22**, 475 (1997).

[7] S. Luo, W. Luo, J.D. Clewley, T. Flanagan, L.A. Wade, J. Alloys Comp. **231**, 467 (1995).

[8] B. Rożdżyńska-Kiełbik, W. Iwasieczko, H. Drulis, V.V. Pavlyuk, H. Bala, J. Alloys Comp. **298**, 237 (2000).

[9] K. Giza, W. Iwasieczko, H. Bala, V.V. Pavlyuk, H. Drulis, Int. J. Hydr. Energy **34**, 915 (2009).

[10] C. Witham, A. Hightower, B. Fultz, B.V. Ratnakumar, R.C. Bowman Jr., J. Electrochem. Soc. **144**, 3758 (1997).

[11] R.C. Bowman, C. Witham, B. Fultz, B.V. Ratnakumar, T.W. Ellis, I.E. Anderson, J. Alloys Comp. **253**, 613 (1997).

[12] A.S. Pratt, D.B. Willey, I.R. Harris, Platinum Metals Rev. **43**, 50 (1999).

[13] C. Iwakura, M. Miyamoto, H. Inoue, M. Matsuoka, Y. Fukumoto, J. Alloys Comp. **259**, 129 and 132 (1997).

[14] A. Vaskelis, R. Juskenas, J. Jciauskiene, Electrochim Acta **43**, 1061 (1998).

[15] B. Rożdżyńska-Kiełbik, A.V. Gaudyn, K. Giza, Międzynarodowa Konferencja Naukowa, Nowe technologie i osiągnięcia w metalurgii i inżynierii materiałowej, 527 Częstochowa (2007).

[16] K. Giza, H. Bala, B. Rożdżyńska-Kiełbik, Inż. Materiałowa **29**, 1025 (2008).

[17] I. Kukuła, H. Bala, Ochr. przed Korozją **53**, 4-5, 225 (2010).

[18] C. Iwakura, K. Fukuda, H. Senoh, H. Inoue, M. Matsuoka, Y. Yamamoto, Electrochim. Acta **43**, 2041 (1998).

[19] I. Kukuła, H. Bala, Ochr. przed Korozją **53**, 11 (2010).

[20] C. Khaldi, H. Mathlouthi, J. Lamloumi, A. Percheron-Guegan, Int. J. Hydr. Energy **29**, 307 (2004).

[21] T. Nishina, H. Ura, J. Uchida, J. Electrochem. Soc. **143**, 1287 (1996) and **144**, 1273 (1997).

[22] G. Zheng, B.N. Popov, R.E. White, J. Electrochem. Soc. **142**, 8, 2695 (1995).

[23] P.J. Schneider, Conduction Heat Transfer, Addison-Wesley, Cambridge (1955).

[24] J. Crank, The Mathematics of Diffusion, Clarendom Press, Oxford (1975).

[25] J.G. Willems, Philips J. Res. **39**, 1 (1984).

[26] H. Pan, Y. Chen, C. Wang, J.X. Ma, C.P. Chen, Q.D. Wang, Electrochim. Acta **44**, 2263 (1999).

[27] M.H.J. Van Rijswick, In Hydrides for Energy Storage, A.F. Anderesen, A.J. Maeland, Editors, p. 261, Pergamon Press, Oxford (1978).

[28] K. Giza, H. Bala, E. Owczarek, B. Rożdżyńska-Kiełbik, V.V. Pavlyuk, Ochr. przed Korozją **50**, 11s/A, 162 (2007).

[29] I. Kukuła, H. Bala, B. Marciniak, V.V. Pavlyuk, Ochr. przed Korozją **52**, 4-5, 202 (2009).

[30] Y. Li, S. Han, J. Li, X. Zhu, L. Hu, J. Alloys Comp. **458**, 357 (2008).